

# Directional excitation of graphene surface plasmons

Fangli Liu<sup>\*</sup> and Y. D. Chong<sup>†</sup>

*School of Physical and Mathematical Sciences and Centre for Disruptive Photonic Technologies,  
Nanyang Technological University, 21 Nanyang Link, 637371, Singapore*

Cheng Qian

*School of Computer Engineering, Nanyang Technological University, Nanyang Avenue, 639798, Singapore*

We propose a scheme to directionally couple light into graphene plasmons by placing a graphene sheet on a magneto-optical substrate. When a magnetic field is applied parallel to the surface, the graphene plasmon dispersion relation becomes asymmetric in the forward and backward directions. It is possible to achieve unidirectional excitation of graphene plasmons with normally incident illumination by applying a grating to the substrate. The directionality can be actively controlled by electrically gating the graphene, or by varying the magnetic bias. This scheme may have applications in graphene-based opto-electronics and sensing.

PACS numbers:

*Introduction.*— Since the first exfoliation of graphene ten years ago [1], this two-dimensional material has attracted tremendous research interest, due to its unique electronic [2], mechanical [3], optical [4] and thermal properties [5]. Its high carrier mobility at room temperature makes it a promising material for post-silicon electronics, as well as for photonic and opto-electronic devices. Although an isolated layer of intrinsic graphene interacts rather weakly with light (absorbing only  $\sim 2.3\%$  of the incident intensity, independent of frequency [4]), the interaction can be enhanced by external cavity resonances [6–8], or by plasmonic resonances of the graphene surface itself [9–12]. The latter approach, which is the domain of the emerging field of “graphene plasmonics”, produces operating frequencies in the technologically-relevant terahertz to mid-infrared range. Compared to conventional metal surface plasmons, graphene surface plasmons are subject to lower propagation losses [13–15]. They also have the virtue of being highly tunable, via electrostatic or chemical doping of the graphene layer [10, 11].

This paper investigates the interesting possibility of *directionally* exciting graphene surface plasmons with the aid of a magneto-optical substrate. In order for graphene plasmons to be excited by external illumination, surface modulations are typically needed for wave-vector matching. One approach is to pattern the graphene into nano-ribbons, which localizes the plasmon resonances [10–12]. Alternatively, propagating graphene plasmons can be excited by patterning gratings into the substrate [16], or by applying elastic vibrations to the graphene [17, 18]. In principle, very high coupling efficiencies (on the order of 50%) can be achieved [17]. However, these methods excite plasmons in both directions along the grating. For numerous switching applications, it would be useful to be able to control the propagation direction of the plasmons. In the literature on conventional surface plasmons, several methods for directional excitation have recently been explored [19–25]. However, it is challenging

to apply most of these methods [21–25] to graphene plasmons, due to graphene’s two-dimensional nature, as well as the technical difficulty of patterning a meta-surface onto graphene without harming the optical sheet conductivity by edge scattering [12].

The system we investigate consists of a graphene layer on a magneto-optical substrate magnetized parallel to the surface. Unlike other recent papers on magnetic graphene plasmons [26–28], we do not magnetize the graphene sheet perpendicular to the plane, which would induce Landau levels and an off-diagonal current response. As discussed below, such schemes do not lead to the desired phenomenon of directional in-plane excitation. In the present system, the propagation of the graphene plasmon is made nonreciprocal by the penetration of the plasmon mode into the magneto-optical substrate, which is magnetically biased parallel to the surface and perpendicular to the direction of propagation. This configuration is reminiscent of the work of Yu *et al.* [29], who showed that a surface plasmon at the interface between a dielectric and a magnetic metal (likewise biased parallel to the surface) exhibits an asymmetric dispersion relation. Remarkably, because that system has a dispersion relation with a frequency cutoff, it acts as a unidirectional plasmonic waveguide over a finite frequency bandwidth below the cutoff. In the case of graphene plasmons, it is a well-known fact that no such cutoff exists [13]. Nonetheless, directionality can be enforced at *specific* frequencies by the application of a grating, e.g. with a modulated substrate surface. Light incident at an appropriately-chosen frequency can thus excite graphene plasmons in one direction. For a fixed operating frequency, it is even possible to actively reverse the direction of excitation, either by switching the magnetic field direction, or (more interestingly) by varying the doping level of the graphene layer. Such a device may have applications in graphene-based opto-electronic and photonic devices, such as optical absorbers, nano-sensors, and molecular detectors.

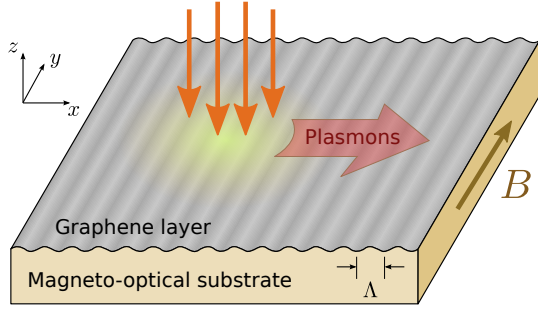


FIG. 1: Schematic of the device under investigation. A graphene sheet lies on a grated magnetic-optical substrate which has period  $\Lambda$ . A magnetic field is applied along the  $\hat{y}$  direction, parallel to the surface and perpendicular to the normal of the grating. Normally incident monochromatic light excites surface plasmons propagating in a single direction.

*Asymmetric Dispersion Relation.*— Consider a graphene sheet lying on an magnetic-optical substrate, as shown schematically in Fig. 1. A grating is etched onto the surface, with period  $\Lambda$ . If the modulation is sufficiently weak, it will not significantly affect the dispersion relation of surface plasmon modes [30]. Thus, we can derive the plasmon dispersion by taking the limit of zero modulation (i.e., a flat surface). When a magnetic field applied in the  $\hat{y}$  direction, the relative dielectric constant of the substrate (medium 1) is

$$\vec{\epsilon} = \begin{bmatrix} \epsilon_1 & 0 & i\alpha \\ 0 & \epsilon_{\parallel} & 0 \\ -i\alpha & 0 & \epsilon_1 \end{bmatrix}. \quad (1)$$

Here,  $\epsilon_1$  and  $\epsilon_{\parallel}$  are the dielectric components perpendicular to and parallel to the magnetization;  $\alpha$  is the magneto-optical component. Note that the magnetic field is applied in  $y$  direction (parallel to the surface), so it does not split the electronic states into Landau levels, unlike the case where the magnetic field is applied through the graphene sheet [26–28]. Above the graphene, the dielectric constant is  $\epsilon_2$  (medium 2). The graphene layer has isotropic sheet conductivity  $\sigma$ .

We look for surface plasmon modes where the electric and magnetic fields in medium 1 and 2 have the form

$$\vec{E}_j(x, z) = (E_{jx}, 0, E_{jz})e^{iqx}e^{-k_j|z|} \quad (2)$$

$$\vec{H}_j(x, z) = (0, H_{jy}, 0)e^{iqx}e^{-k_j|z|}, \quad (3)$$

where  $q$  denotes the wavevector in the  $\hat{x}$  direction,  $k_j$  is the decay constant in the  $z$  direction, for medium index  $j = 1, 2$ . We plug these expressions into Maxwell's equations, assume all the time-dependent fields are harmonic with frequency  $\omega$ , and impose the boundary conditions  $E_{1x} = E_{2x}$  and  $B_{1y} = B_{2y} - \sigma E_{1x}$  along the graphene layer. The resulting dispersion relation is:

$$\frac{\epsilon_2}{k_2} + \frac{\epsilon_1^2 - \alpha^2}{k_1\epsilon_1 + q\alpha} + \frac{i\sigma}{\omega\epsilon_0} = 0, \quad (4)$$

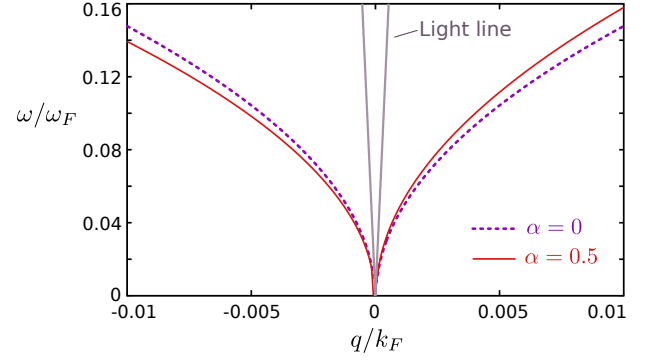


FIG. 2: Dispersion relations for graphene surface plasmons on magneto-optical substrates, calculated numerically from Eqs. (4)–(7). The wavenumber and frequency are respectively scaled relative to  $k_F$  and  $\omega_F$ , the Fermi wavenumber and frequency in the graphene sheet (which are both proportional to the Fermi level). We assume a Fermi velocity of  $10^6 \text{ms}^{-1}$  and  $\tau = 0$  in the graphene sheet. The relative dielectric constants  $\epsilon_1 = 3$  and  $\epsilon_2 = 1$ , and the magneto-optical parameter  $\alpha$ , are taken to be frequency-independent. For  $\alpha = 0$ , the dispersion relation is symmetric; setting  $\alpha \neq 0$  makes it asymmetric.

where  $\epsilon_0$  is the permittivity of free space and

$$k_1 = \sqrt{q^2 - \left(\frac{\epsilon_1^2 - \alpha^2}{\epsilon_1}\right) \frac{\omega^2}{c^2}} \quad (5)$$

$$k_2 = \sqrt{q^2 - \epsilon_2 \frac{\omega^2}{c^2}}. \quad (6)$$

Evidently,  $k_1$  and  $k_2$  only depend on the absolute value of  $q$ , and do not depend on the direction of propagation. However, the second term of Eq. (4) has a denominator which involves  $q$  rather than  $q^2$ . This is the source of the magneto-optically induced asymmetry.

Graphene's sheet conductivity can be modeled by [31]

$$\sigma(\omega) = \frac{e^2 E_F}{\pi \hbar^2} \frac{i}{\omega + i/\tau}, \quad (7)$$

where  $E_F$ ,  $\tau$ ,  $\hbar$ , and  $e$  are the doping level, damping time, Planck constant, and electron charge respectively. Fig. 2 shows the asymmetric dispersion relation computed numerically from Eqs. (4)–(7), assuming frequency-independent dielectric components.

We will work in the “non-retarded” regime, where the mode lies well below the light line and is well-confined [13]. For  $1/\tau \ll \omega \ll qc$ , Eqs. (4)–(7) simplify to

$$\omega \approx \sqrt{\frac{e^2 E_F}{\pi \hbar^2 \epsilon_0} \cdot \frac{|q|}{\epsilon_1 + \epsilon_2 \mp \alpha}}, \quad (8)$$

where  $\pm$  denote right and left propagation respectively. For  $\alpha = 0$ , Eq. (8) reduces to the usual square-root dispersion relation for graphene surface plasmons [13]. For  $\alpha \neq 0$ , the dispersion relation is asymmetric; for fixed  $|q|$ ,

there are two different values for  $\omega$ . Note that  $\alpha$ ,  $\epsilon_1$ , and  $\epsilon_2$  can also depend implicitly on  $\omega$ .

From Eq. (8), we obtain the frequency difference ratio

$$\frac{\delta\omega}{\omega_0} \sim \frac{\alpha}{\epsilon_1 + \epsilon_2}, \quad (9)$$

where, for fixed  $|q|$ ,  $\delta\omega$  is the frequency difference between right- and left-moving plasmons. This ratio depends only on the relative strength of the magnetic-optical component in the bulk media. It does not depend on the graphene sheet conductivity, which affects only  $\omega_0$ , the unmagnetized graphene surface plasmon frequency.

For a typical magneto-optical material, the dielectric components defined in (1) can be modeled by [32–34]

$$\epsilon_1(\omega) = \left(1 - \frac{\omega_p^2}{\omega^2 - \omega_c^2}\right) \epsilon_\infty \quad (10)$$

$$\alpha(\omega) = \frac{\omega_p^2 \omega_c}{\omega(\omega^2 - \omega_c^2)} \epsilon_\infty, \quad (11)$$

where  $\epsilon_\infty$  is the limiting permittivity at high frequencies,  $\omega_p$  is the bulk plasma frequency, and  $\omega_c$  is the cyclotron frequency induced by the magnetic bias. Assuming  $\epsilon_2 = 1$  and weak magnetization ( $\omega_c \ll \omega, \omega_p$ ), combining Eqs. (9)–(11) gives

$$\delta\omega \sim \omega_c \cdot \frac{\omega_p^2/\omega_0^2}{\epsilon_\infty^{-1} + 1 - \omega_p^2/\omega_0^2}. \quad (12)$$

It is useful to compare these results to the “magnetic surface plasmon” which occurs at the interface between a dielectric and a magnetic metal [29]. That situation corresponds to setting  $\sigma = 0$  in Eq. (4); in order for a confined state to exist in the absence of the conducting layer, the magneto-optical material must then be metallic ( $\epsilon_1 < 0$ ). In the large- $q$  regime, the magneto-optical frequency difference is found to be  $\delta\omega \sim \omega_c$ , with no leading-order dependence on  $\epsilon_\infty$  or  $\omega_p$ . Because the magnetic surface plasmon’s dispersion relation has a frequency cutoff, propagation becomes unidirectional in a finite frequency range near the cutoff [29]. In the present case, however, the confinement is provided by the graphene layer, and we can take the magneto-optical material to be non-metallic ( $\epsilon_1 > 0$ ); because the dispersion relation has no cutoff, directionality has to be imposed by other means, such as a grating.

*Directional coupling.*— To excite the graphene surface plasmons, we consider applying a weak periodic modulation to the surface of the substrate. The grating couples incident light with transverse wavevector component  $k_0$  to surface plasmons with wave-vector  $k_{\text{spp}} = k_0 \pm 2\pi N/\Lambda$ , where  $\Lambda$  is the grating period and  $N \in \mathbb{Z}^+$ . In the non-retarded regime, the directionality of the incident light has little effect on the coupling since  $k_0 \ll k_{\text{spp}}$  (as indicated in Fig. 2). Henceforth, we assume normal incidence ( $k_0 = 0$ ) for simplicity.

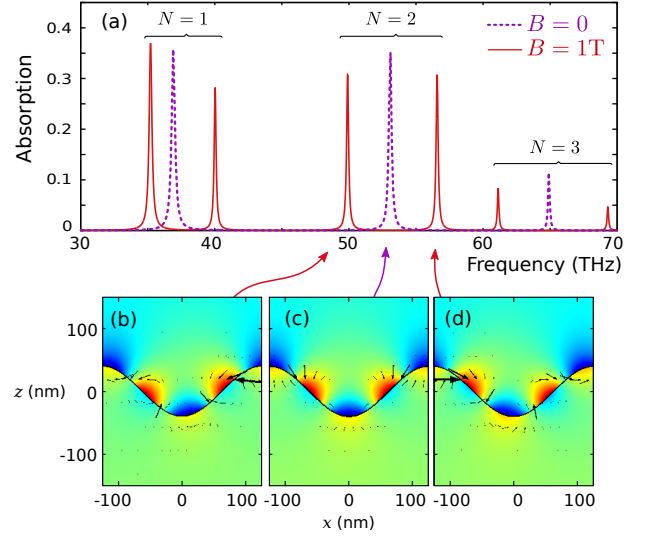


FIG. 3: (a) Absorption spectrum of graphene surface plasmon resonances, obtained by full-wave simulations of the system shown in Fig. 1. With zero applied magnetic field (blue triangles), there is a single absorption peak, corresponding to bi-directional excitation of surface plasmons. With a 1T applied magnetic field (red circles), there are two distinct absorption peaks, corresponding to plasmons propagating with wave-vector  $\pm 2\pi/\Lambda$ , where  $\Lambda$  is the grating period. (b)–(d) Plots of  $H_z$  at each of the resonances, with black arrows indicating the local Poynting vector.

For nonzero magnetic bias, the incident light couples to left- and right-moving surface plasmons at different resonance frequencies. To demonstrate this effect, we perform full-wave finite element simulations of Maxwell’s equations (using the Comsol Multiphysics software package) for the setup of Fig. 1. The results are shown in Fig. 3. For the substrate, we use indium antimonide (InSb), which has been shown to have large magnetic-optical response at terahertz and mid-infrared frequencies [32–34]. Its dielectric tensor components can be modeled by Eqs. (10)–(11), with  $\epsilon_\infty = 15.68$  and  $\omega_c = eB/m^*$  (where  $m^* = 0.014m_e$  is the effective mass). The bulk plasma frequency is given by  $\omega_p^2 = Ne^2/(\epsilon_\infty m^* \epsilon_0)$ , where  $N = 5.5 \times 10^6 \mu\text{m}^{-3}$ . For an operating frequency of 50 THz and magnetic bias of  $B = 1\text{T}$ , this results in  $\epsilon_1 \approx 3$  and  $\alpha \approx 0.5$ . The grating has period  $\Lambda = 250\text{ nm}$  and modulation amplitude 40 nm (note that these length scales are sufficiently large that quantum effects can be safely ignored [35]). To model the graphene sheet, we use a thin layer of thickness  $d \approx 0.3\text{ nm}$  with effective dielectric constant  $\epsilon_{\text{eff}} = 1 + i\sigma/(\epsilon_0 \omega d)$ . The graphene conductivity parameters are taken to be  $E_F = 1\text{ eV}$  and  $\tau = 10^{-12}\text{s}^{-1}$ , in line with typical experimental values for doped graphene on a semiconductor substrate.

In Fig. 3(a), we see that in the absence of an applied magnetic field is applied, there are absorption peaks near 37 THz, 53 THz, 65 THz ..., corresponding to the exci-

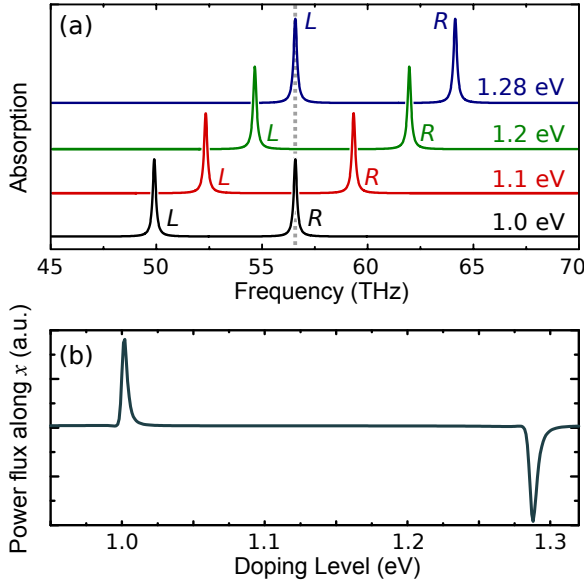


FIG. 4: Active control of plasmon excitation directionality. (a) The resonance peaks, which correspond to left-moving ( $L$ ) and right-moving ( $R$ ) plasmons, can be shifted by tuning the doping level of the graphene layer. Hence, at a fixed operating frequency (vertical dashes), we can excite right-moving plasmons at a 1 eV doping level, or right-moving plasmons at 1.28 eV. (b) The power flux through one unit cell in the  $x$  direction (calculated by integrating the Poynting vector) versus the doping level, for a fixed excitation frequency of 56.6 THz. This confirms that the plasmons propagate to the left and right at 1 eV and 1.28 eV doping levels respectively. These results were obtained from finite-element simulations with all other parameters the same as in Fig. 3.

tation of surface plasmons for different values of  $N$ . The field distribution of  $H_y$  for the  $N = 2$  mode is plotted in Fig. 3(c), showing that it is a tightly-confined surface plasmon mode. The Poynting vectors, indicated by black arrows in this plot, reveal that the mode is symmetric (i.e., zero net energy flow along the  $\hat{x}$  axis). When a magnetic field is applied, each absorption peak splits into two, one below the original frequency and one above, with absorption coefficients comparable to the original peak. The field distributions for the  $N = 2$  modes are plotted in Fig. 3(b) and (d), and the Poynting vectors indicate the modes are directional, transporting energy in the  $-\hat{x}$  and  $+\hat{x}$  directions respectively. When the direction of the applied magnetic field is reversed,  $\alpha$  switches sign. Thus, at a fixed operating frequency, we can actively control the directionality of the excited surface plasmons.

Another interesting way to control the directionality of the excited surface plasmons is to exploit the extraordinary tunability of graphene's electrical properties. The value of  $\omega_F$  in graphene, which enters into the dispersion relation of the surface plasmon via Eq. (8), can be controlled very precisely by electrical doping (or a combination of electrical and chemical doping). In Fig. 4, we

give an example where, at a single operating frequency (56.6 THz), the directionality of the excited surface plasmons can be reversed by switching the doping level from 1 eV to 1.28 eV. This tunability may be useful for applications in switchable plasmonics.

*Discussion.*— The setup we have considered in this paper is different from the one considered in most previous works on magnetic plasmons in graphene, where the magnetic field is applied perpendicular to the plane of the graphene sheet. In that latter setup, the graphene bandstructure forms Landau levels [26–28], resulting in a complicated splitting of the plasmon frequencies [36]. However, this splitting only affects the transmission coefficient of circular polarized incident light; it does not excite the plasmon in a specific *in-plane* direction, which is the phenomenon we are interested in. Recently, Xiao *et al* have studied a setup where the magnetic field is applied in-plane [37]. However, they treated the case of a stack of graphene sheets several microns thick, and considered the magneto-optical effect occurring in that stack, in a manner directly analogous to the magnetic surface plasmons of Ref. [29]. Such a scheme is not practically realizable or relevant to the case of monolayer graphene. In our work, the magneto-optical effect is due to the substrate material, not the graphene layer.

In our simulations, we have chosen to focus on the simplest mechanism for coupling incident light to the surface plasmons, i.e. by modulating the substrate surface. The properties of graphene have previously been shown to be strongly affected by the choice of substrate [38–40], and the feasibility of patterning graphene on a magneto-optical substrate, such as InSb, is an open experimental question. We emphasize, however, that details about the implementation of the grating mainly affect the coupling efficiency, and largely do not alter our analysis of the dispersion relation of magneto-optical graphene surface plasmons. For instance, one might instead deposit a dielectric grating on top of the graphene, or use graphene ribbons instead of a contiguous graphene sheet [10].

In conclusion, we have presented a simple scheme for directionally exciting graphene surface plasmons, based on the asymmetry in the surface plasmon dispersion relation due to a magneto-optical substrate. The directionality can be actively controlled, such as by electrically gating the graphene layer. This proposal may be useful as the coupling mechanism for more complex graphene plasmonic devices. It would also be interesting to explore the possibility of using an alternative conducting material, such as a metallic thin film, in place of the graphene; the surface plasmons which arise in such dielectric/thin metal/magneto-optical dielectric structures may have useful applications outside the context of graphene-based technologies.

*Acknowledgements.*— We thank X. Lin and Q. J. Wang for helpful discussions. This research was supported by the Singapore National Research Foundation under grant



No. NRFF2012-02, and by the Singapore MOE Academic Research Fund Tier 3 grant MOE2011-T3-1-005.

---

\* Electronic address: [liuf0025@e.ntu.edu.sg](mailto:liuf0025@e.ntu.edu.sg)

† Electronic address: [yidong@ntu.edu.sg](mailto:yidong@ntu.edu.sg)

- [1] K. S. Novoselov, A. K. Geim, S. V. Morozov, D. Jiang, Y. Zhang, S. V. Dubonos, I. V. Grigorieva and A. A. Firsov, *Science* **306**, 666 (2004).
- [2] A. H. Castro Neto, F. Guinea, N. M. R. Peres, K. S. Novoselov, and A. K. Geim, *Rev. Mod. Phys.* **81**, 109 (2009).
- [3] C. Lee, X. Wei, J. W. Kysar and J. Hone, *Science* **321**, 385 (2008).
- [4] A. B. Kuzmenko, E. van Heumen, F. Carbone, and D. van der Marel, *Phys. Rev. Lett.* **100**, 117401 (2008).
- [5] A. A. Balandin, *Nature Mat.* **10**, 569 (2011).
- [6] M. Engel, M. Steiner, A. Lombardo, A. C. Ferrari, H. v. Loehneysen, P. Avouris, and R. Krupke, *Nature Commun.* **3**, 906 (2012).
- [7] M. Furchi, A. Urich, A. Pospischil, G. Lilley, K. Unterrainer, H. Detz, P. Klang, A. M. Andrews, W. Schrenk, G. Strasser, and T. Mueller, *Nano Lett.* **12**, 2773 (2012).
- [8] F. Liu, Y. D. Chong, S. Adam and M. Polini, *2D Mat.* **1**, 031001 (2014).
- [9] E. H. Hwang and S. Das Sarma, *Phys. Rev. B* **75**, 205418 (2007).
- [10] L. Ju, B. Geng, J. Horng, C. Girit, M. Martin, Z. Hao, H. A. Bechtel, X. Liang, A. Zettl, Y. R. Shen, and F. Wang, *Nature Nano.* **6**, 630, (2011).
- [11] H. Yan, X. Li, B. Chandra, G. Tulevski, Y. Wu, M. Freitag, W. Zhu, P. Avouris and F. Xia, *Nature Nano.* **7** 330 (2012).
- [12] H. Yan, T. Low, W. Zhu, Y. Wu, M. Freitag, X. Li, F. Guinea, P. Avouris and F. Xia, *Nature Phot.* **7** 394 (2013).
- [13] M. Jablan, H. Buljan, and M. Soljačić, *Phys. Rev. B* **80**, 245435 (2009).
- [14] F. H. L. Koppens, D. E. Chang, and F. J. G. de Abajo, *Nano Lett.* **11**, 3370 (2011).
- [15] Z. Fei, A. S. Rodin, G. O. Andreev, W. Bao, A. S. McLeod, M. Wagner, L. M. Zhang, Z. Zhao, M. Thiemens, G. Dominguez, M. M. Fogler, A. H. Castro Neto, C. N. Lau, F. Keilmann, and D. N. Basov, *Nature* **487**, 82 (2012).
- [16] F. Aires and N. M. R. Peres, *Phys. Rev. B* **86**, 205401 (2012).
- [17] M. Farhat, S. Guenneau, and H. Bağcı, *Phys. Rev. Lett.* **111**, 237404 (2013).
- [18] J. Schiefele, J. Pedrós, F. Sols, F. Calle, and F. Guinea, *Phys. Rev. Lett.* **111**, 237405 (2013).
- [19] A. G. Curto, G. Volpe, T. H. Taminiau, M. P. Kreuzer, R. Quidant, N. F. van Hulst, *Science* **329** 930 (2010).
- [20] T. H. Taminiau, F. D. Stefani, N. F. van Hulst, *Opt. Ex.* **16**, 10858 (2008).
- [21] T. Xu, Y. Zhao, D. Gan, C. Wang, C. Du and X. Luo, *Appl. Phys. Lett.* **92**, 101501 (2008).
- [22] X. Li, Q. Tan, B. Bai and G. Jin, *Appl. Phys. Lett.* **98**, 251109 (2011).
- [23] J. Lin, J. P. B. Mueller, Q. Wang, G. Yuan, N. Antoniou, X.-C. Yuan, and F. Capasso, *Science* **340** 331 (2013).
- [24] F. J. Rodriguez-Fortuño, G. Marino, P. Ginzburg, D. O'Connor, A. Martínez, G. A. Wurtz, and A. V. Zayats, *Science* **340**, 328 (2013).
- [25] L. Huang, X. Chen, B. Bai, Q. Tan, G. Jin, T. Zentgraf, and S. Zhang, *Light: Sci. & Appl.* **2** e70 (2013).
- [26] Y. Zhang, Z. Jiang, J. P. Small, M. S. Purewal, Y.-W. Tan, M. Fazlollahi, J. D. Chudow, J. A. Jaszczak, H. L. Stormer, and P. Kim, *Phys. Rev. Lett.* **96**, 136806 (2006).
- [27] I. Crassee, J. Levallois, A. L. Walter, M. Ostler, A. Bostwick, E. Rotenberg, T. Seyller, D. van der Marel, and A. B. Kuzmenko, *Nature Phys.* **7**, 48 (2011).
- [28] M. L. Sadowski, G. Martinez, M. Potemski, C. Berger, and W. A. de Heer, *Phys. Rev. Lett.* **97**, 266405 (2006).
- [29] Z. Yu, G. Veronis, Z. Wang, and S. Fan, *Phys. Rev. Lett.* **100**, 023902 (2008).
- [30] A. Y. Nikitin, S. A. Maier and L. Martin-Moreno, *J. Opt.* **15**, 110201 (2013).
- [31] Y. V. Bludov, A. Ferreira, N. M. R. Peres, M. I. Vasilevskiy, *Int. J. Mod. Phys. B* **27**, 1341001 (2013).
- [32] J. G. Rivas, C. Janke, P. H. Bolivar, and H. Kurz, *Opt. Ex.* **13**, 847 (2005).
- [33] B. Hu, Q. J. Wang, and Y. Zhang, *Opt. Ex.* **20** 10071 (2012).
- [34] B. Hu, Q. J. Wang, and Y. Zhang, *Opt. Lett.* **37** 1895 (2012).
- [35] S. Thongrattanasiri, A. Manjavacas, and F. J. G. de Abajo, *ACS Nano* **6** 1766 (2012).
- [36] H. Yan, Z. Li, X. Li, W. Zhu, P. Avouris, and F. Xia, *Nano Lett.* **12**, 3766 (2012).
- [37] X. Lin, Y. Xu, B. Zhang, R. Hao, H. Chen and E. Li, *N. J. Phys.* **15** 113003 (2013).
- [38] C. R. Dean, A. F. Young, I. Meric, C. Lee, L. Wang, S. Sorgenfrei, K. Watanabe, T. Taniguchi, P. Kim, K. L. Shepard, and J. Hone, *Nature Nano.* **5** 722 (2010).
- [39] J. C. Jang, S. Adam, J.-H. Chen, E. D. Williams, S. Das Sarma, and M. S. Fuhrer, *Phys. Rev. Lett.* **101**, 146805 (2008).
- [40] Z.-Y. Ong and E. Pop, *Phys. Rev. B* **84**, 075471 (2011).